Tokyo Climate Center, Japan Meteorological Agency

TCC News

No. 54 Autumn 2018

Contents Page

El Niño Outlook (November 2018 – May 2019)

El Niño conditions are considered to have been present in the equatorial Pacific in October and are likely (70%) to continue until boreal spring. (Article based on the El Niño outlook issued on 9 November 2018.)

El Niño/La Niña

The NINO.3 SST deviation was +0.9°C in October, and SSTs for the month were above normal in most of the equatorial Pacific (Figures 1 and 3 (a)). Subsurface temperatures were also above normal in most of the equatorial Pacific (Figures 2 and 3 (b)). Atmospheric convective activity was near normal near the date line over the equatorial Pacific, while easterly winds in the lower troposphere (trade winds) were below normal over the central equatorial Pacific. As these oceanic and atmospheric conditions indicate common features of past El Niño events, El Niño conditions are considered to be present in the equatorial Pacific.

The subsurface warm waters are expected to support ongoing higher-than-normal SSTs in the eastern part of the equatorial Pacific. JMA's El Niño prediction model suggests that the NINO.3 SST will be above normal throughout the prediction period (Figure 4). Based on this prediction and the observations described above, there is a probability of over 70% that the five-month running mean NINO.3 SST will be +0.5°C or above in boreal winter and beyond (Figure 5). In conclusion, there is a 70% probability that El Niño conditions will continue until boreal spring.

Western Pacific and Indian Ocean

The area-averaged SST in the tropical western Pacific (NINO.WEST) region was near normal in October. It is likely that the value will be below normal until boreal spring. The area-averaged SST in the tropical Indian Ocean (IOBW) region was below normal in October. It is likely that the value will be approximately near normal in boreal autumn and above normal or near normal from boreal winter to spring.

(Shiro Ishizaki, Climate Prediction Division)

* The SST normal for the NINO.3 indices (5°S – 5°N, 150°W – 90°W) is defined as an monthly average over the latest sliding 30-year period (1988-2017 for this year).
* The SST normals for the NINO.WEST indices (Eq. – 15°N, 130°E – 150°E) and the IOBW indices (20°S – 20°N, 40°E – 100°E) are defined as linear extrapolations with respect to the latest sliding 30-year period, in order to remove the effects of significant long-term warming trends observed in these regions.

(a) (b)

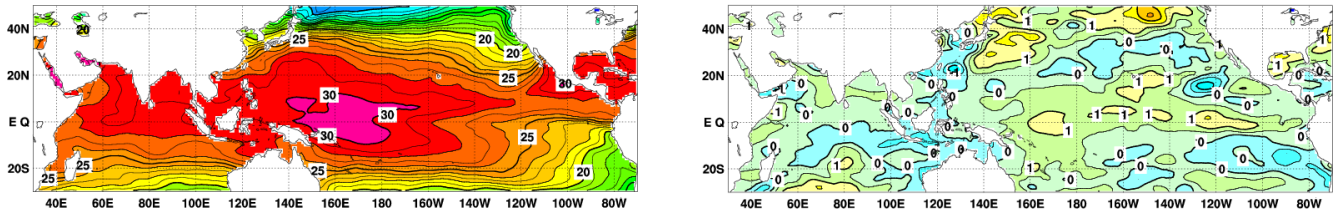

Figure 1 Monthly mean (a) sea surface temperatures (SSTs) and (b) SST anomalies in the Indian and Pacific Ocean areas for October 2018
The contour intervals are 1˚C in (a) and 0.5˚C in (b). The base period for the normal is 1981 – 2010.

(a) (b)

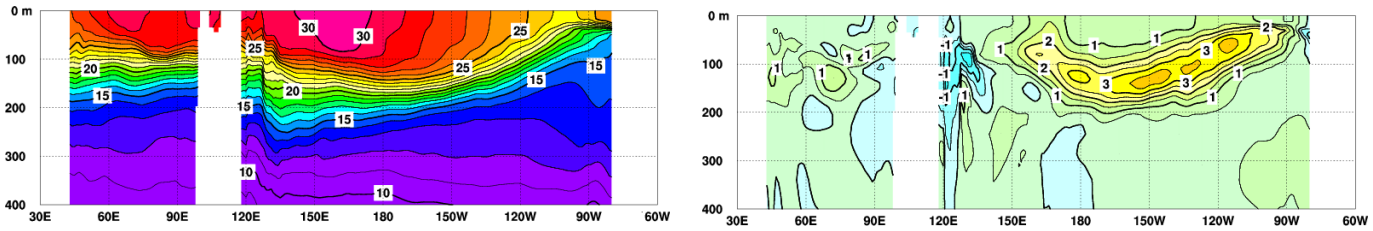

Figure 2 Monthly mean depth-longitude cross sections of (a) temperatures and (b) temperature anomalies in the equatorial Indian and Pacific Ocean areas for October 2018

The contour intervals are 1˚C in (a) and 0.5˚C in (b). The base period for the normal is 1981 – 2010.

(a) (b)

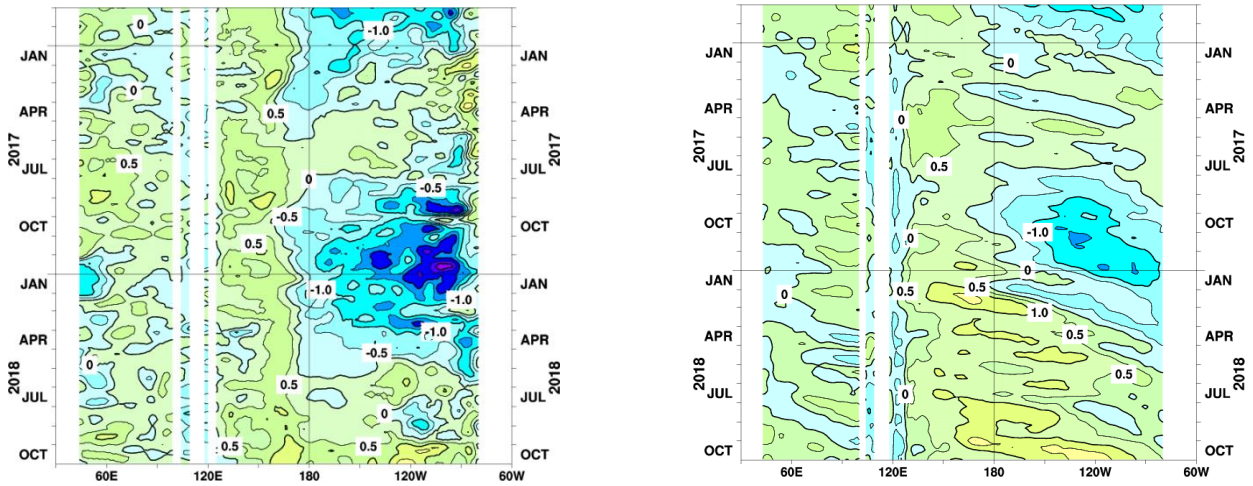

Figure 3 Time-longitude cross sections of (a) SST and (b) ocean heat content (OHC) anomalies along the equator in the Indian and Pacific Ocean areas

OHCs are defined here as vertical averaged temperatures in the top 300 m. The base period for the normal is 1981 – 2010.

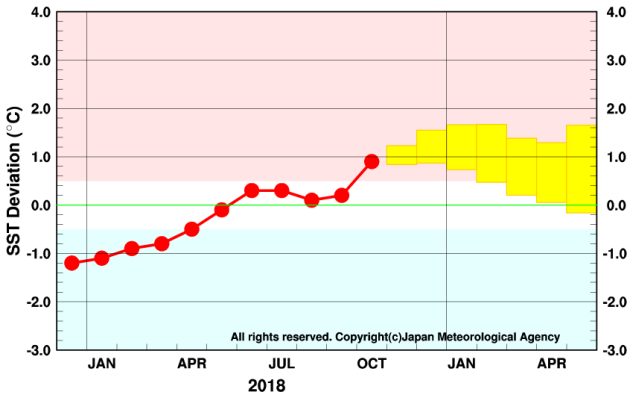

Figure 4 Outlook of NINO.3 SST deviation produced by the El Niño prediction model

This figure shows a time series of monthly NINO.3 SST deviations. The thick line with closed circles shows observed SST deviations, and the boxes show the values produced for up to six months ahead by the El Niño prediction model. Each box denotes the range into which the SST deviation is expected to fall with a probability of 70%.

YEAR	MONTH	mean period		
2018	SEP	JUL2018–NOV2018	70	30
	OCT	AUG2018–DEC2018	90	10
	NOV	**SEP2018–JAN2019**	90	10
	DEC	**OCT2018–FEB2019**	80	20
2019	**JAN**	**NOV2018–MAR2019**	80	20
	FEB	**DEC2018–APR2019**	70	30
	MAR	**JAN2019–MAY2019**	70	30

El Niño ENSO neutral La Niña

Figure 5 ENSO forecast probabilities based on the El Niño prediction model

Red, yellow and blue bars indicate probabilities that the five-month running mean of the NINO.3 SST deviation from the latest sliding 30-year mean will be +0.5°C or above (El Niño), between +0.4 and -0.4°C (ENSO-neutral) and -0.5°C or below (La Niña), respectively. Regular text indicates past months, and bold text indicates current and future months.

JMA's Seasonal Numerical Ensemble Prediction for Winter 2018/2019

Based on JMA's seasonal ensemble prediction system, sea surface temperature (SST) anomalies are predicted to be above normal in the equatorial Pacific during boreal winter 2018/2019, suggesting El Niño conditions. In association with these conditions, active convection is predicted over the equatorial Pacific, while inactive convection is predicted over the region from the Bay of Bengal across the Indochina Peninsula and the South China Sea to the Philippines. Positive anomalies over Japan and negative anomalies over the sea off the western coast of North America are predicted in association with the positive phase of the PNA teleconnection.

1. Introduction

This article outlines JMA's dynamical seasonal ensemble prediction for boreal winter 2018/2019 (December – February, referred to as DJF), which was used as a basis for JMA's operational cold-season outlook issued on 21 November 2018. The outlook is based on the seasonal ensemble prediction system of the Coupled Atmosphere-ocean General Circulation Model (CGCM). See the column below for system details.

Section 2 outlines global SST anomaly predictions, and Section 3 describes the associated circulation field predictions for the tropics and sub-tropics. Finally, the circulation fields predicted for the mid- and high-latitudes of the Northern Hemisphere are discussed in Section 4.

2. SST anomalies

Figure 6 shows predicted SSTs (contours) and related anomalies (shading) for DJF. For SST conditions in the tropical Pacific, above-normal anomalies are predicted in the equatorial Pacific, suggesting El Niño conditions. Conversely, below-normal anomalies are predicted in and around the sea east of Philippines. Meanwhile, near-normal SST conditions are predicted in the Indian Ocean.

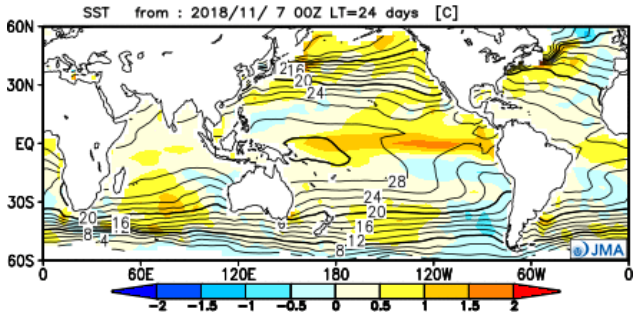

Figure 6 Predicted SSTs (contours) and SST anomalies (shading) for December–February 2018/2019 (ensemble mean of 51 members)

3. Prediction for the tropics and sub-tropics

Figure 7 (a) shows predicted precipitation (contours) and related anomalies (shading) for DJF. Above-normal anomalies are predicted over the equatorial Pacific in association with warmer-than-normal SSTs, while below-normal anomalies are predicted over the Philippines in association with colder-than-normal SSTs.

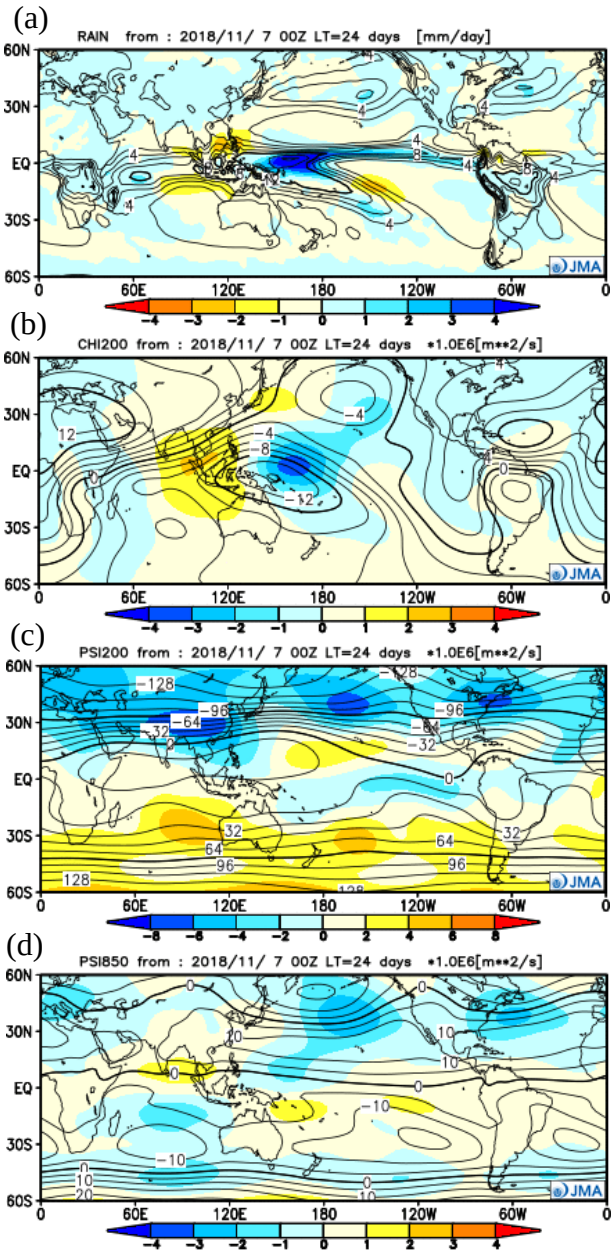

Figure 7 Predicted atmospheric fields from 60°N – 60°S for December–February 2018/2019 (ensemble mean of 51 members)

(a) Precipitation (contours) and anomaly (shading). The contour interval is 2 mm/day.

(b) Velocity potential at 200 hPa (contours) and anomaly (shading). The contour interval is 2×10^6 m^2/s.

(c) Stream function at 200 hPa (contours) and anomaly (shading). The contour interval is 16×10^6 m^2/s.

(d) Stream function at 850 hPa (contours) and anomaly (shading). The contour interval is 5×10^6 m^2/s.

Figure 7 (b) shows predicted velocity potential (contours) and related anomalies (shading) at the upper troposphere (200 hPa) for DJF. Positive (i.e., convergent) anomalies are predicted over the region from the Bay of Bengal across the Indochina Peninsula to the South China Sea. Conversely, negative (i.e., divergent) anomalies are predicted over the equatorial Pacific in association with precipitation.

Figure 7 (c) shows predicted stream functions (contours) and related anomalies (shading) at the upper troposphere (200 hPa) for DJF. Negative (i.e., cyclonic) anomalies are predicted in the most of the Northern Hemisphere, indicating a southward-shift tendency for the subtropical jet stream. Focusing on the strength of negative anomalies, cyclonic anomalies are expected over China in association with suppressed convection in and around the South China Sea and the Philippines. Conversely, equatorially symmetric positive (i.e., anticyclonic) anomalies are predicted over the eastern part of the tropical Pacific in association with El Niño conditions.

Figure 7 (d) shows predicted stream functions (contours) and related anomalies (shading) at the lower troposphere (850 hPa) for DJF. Negative (i.e., cyclonic) anomalies are seen over the sea off the western coast of North America in association with the positive phase of the Pacific North America (PNA) teleconnection as clearly observed during past El Niño events. Conversely, Positive (i.e., anticyclonic) anomalies are predicted in and around the Bay of Bengal in association with lighter-than-normal precipitation.

4. Prediction for the mid- and high- latitudes of the Northern Hemisphere

Figure 8 (a) shows predicted geopotential heights (contours) and related anomalies (shading) at 500 hPa for DJF. Positive anomalies are predicted over most of the Northern Hemisphere in association with global warming trends and El Niño conditions. Large negative anomalies are seen over the sea off the western coast of North America in association with the positive phase of the PNA teleconnection.

Figure 8 (b) shows predicted sea level pressure (contours) and related anomalies (shading) for DJF. Positive anomalies over Japan and negative anomalies over the sea off the western coast of North America are predicted in association with the positive phase of the PNA teleconnection. Meanwhile, small positive anomalies are also predicted over China and Siberia, suggesting a slightly stronger-than-normal Siberian High. However, this should be interpreted with caution due to significant uncertainty.

(Takuya Komori, Tokyo Climate Center)

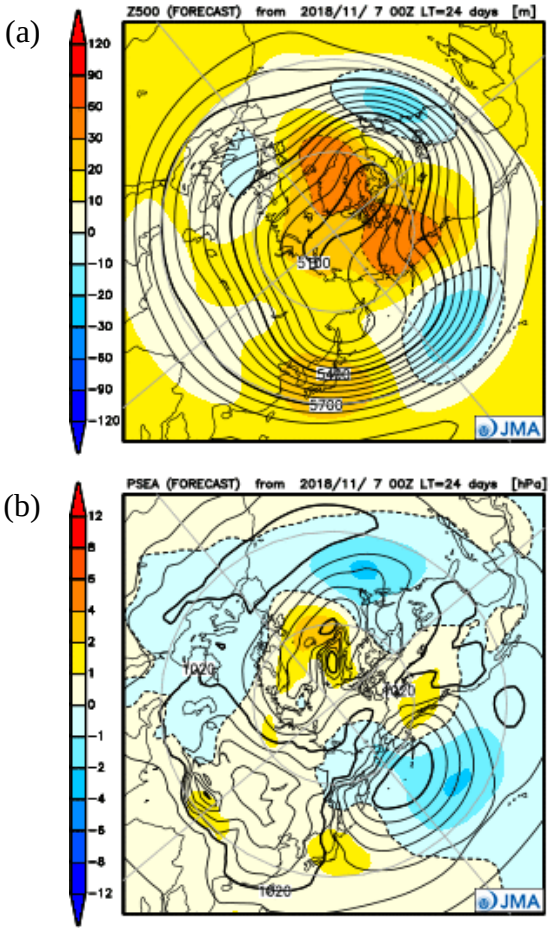

Figures 8 Predicted atmospheric fields from 20°N – 90°N for December–February 2018/2019 (ensemble mean of 51 members)
(a) Geopotential height at 500 hPa (contours) and anomaly (shading). The contour interval is 60 m.
(b) Sea level pressure (contours) and anomaly (shading). The contour interval is 4 hPa.

JMA's Seasonal Ensemble Prediction System

JMA operates a seasonal Ensemble Prediction System (EPS) using the Coupled atmosphere-ocean General Circulation Model (CGCM) to make seasonal predictions beyond a one-month time range. The EPS produces perturbed initial conditions by means of a combination of the initial perturbation method and the lagged average forecasting (LAF) method. The prediction is made using 51 members from the latest four initial dates (13 members are run every 5 days). Details of the prediction system and verification maps based on 30-year hindcast experiments (1981–2010) are available at https://ds.data.jma.go.jp/tcc/tcc/products/model/.

Cold Season Outlook for Winter 2018/2019 in Japan

JMA issued its outlook for the coming winter (December 2018 – February 2019) over Japan in September and updated it in November based on the Agency's seasonal Ensemble Prediction System (EPS). This article outlines the outlook update of 21 November.

1. Outlook summary (Figure 9)

- In eastern/western Japan and Okinawa/Amami, seasonal mean temperatures are expected to exhibit above-normal tendencies and snowfall amounts for the Sea of Japan side are expected to exhibit below-normal tendencies due to a weaker-than-normal winter monsoon.
- Seasonal precipitation amounts in Okinawa/Amami are expected to exhibit above-normal tendencies due to low-pressure systems and fronts
- The intensity of the winter monsoon in northern Japan is expected to be normal, and seasonal mean temperatures, precipitation and snowfall amounts are expected to be near normal.

2. Outlook background

Figure 10 highlights expected large-scale oceanic/atmospheric characteristics for winter. An outline of the background to the outlook is given below.

- El Niño conditions are likely to continue through the coming winter. In association, sea surface temperatures (SSTs) are expected to be above normal in the equatorial Pacific.
- In association with the expected SST anomalies in the tropics, convection will be enhanced over the equatorial Pacific and suppressed from the eastern Indian Ocean to the Maritime Continent.
- In upper circulation fields, the subtropical jet stream is expected to shift southward over the Eurasian continent and meander northward around Japan. In association, cold air inflow toward eastern/western Japan and Okinawa/Amami is expected to be weaker than normal, and Okinawa/Amami is expected to experience low-pressure systems and fronts.
- Upper-level cyclonic circulation anomalies to the northeast of Japan are expected as part of the Pacific North America (PNA) teleconnection pattern in response to the above-mentioned convective activity. In association, the Aleutian Low is expected to be more active than normal, especially in its eastern part, and northern Japan is expected to be affected by the winter monsoon to the normal extent.
- In lower circulation fields, weak southerly wind anomalies to the south of Japan are expected in response to inactive convection around the Maritime Continent. These anomalies could bring humid air to Okinawa/Amami and the Pacific side of the country.
- The expected warmer climatic conditions are consistent with the prevailing El Niño situation. Meanwhile, as the predicted SST anomaly pattern shows a slight westward shift compared to typical El Niño years, convective activity and related atmospheric response may also be shifted westward.
- Overall temperatures in the troposphere are expected to be above-normal over the Northern Hemisphere in association with the prevailing long-term trend.

(Hiroshi Ohno, Climate Prediction Division)

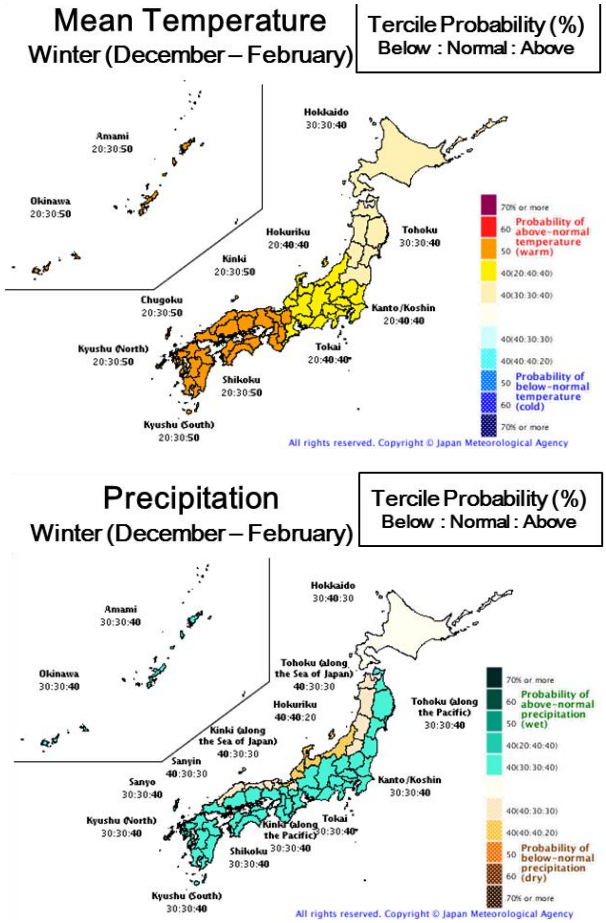

Figure 9 Outlook for winter 2018/2019 temperature (above) and precipitation (below) probability in Japan

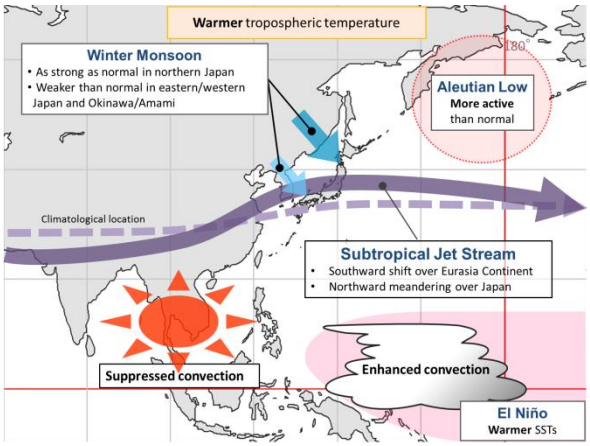

Figure 10 Conceptual diagram showing expected large-scale ocean/atmosphere characteristics for winter 2018/2019

Summary of the 2018 Asian Summer Monsoon

1. Precipitation and temperature

CLIMAT report data detailing the four-month mean temperature for the monsoon season (June – September) show anomalies of more than 1°C above the normal from Japan to central China, in the southern part of Central Siberia and across areas in and around western Pakistan, while values of 1°C and below are seen for parts of western China and from southern Myanmar to western Thailand (Figure 11). From June to August in particular, higher-than-normal temperatures have persisted around the mid-latitude band from 25°N to 45°N, with record seasonal mean temperatures in eastern Japan (the highest since 1946), South Korea (1973) and China (1961). New daily maximum temperatures were also recorded in Japan (41.1°C, Kumagaya, July 23) and South Korea (41.0°C, Hongcheon, August 1).

Four-month total precipitation amounts for the same period were more than 140% of the normal in Hokkaido and western regions of Japan, in and around northern China, from western China to northwestern India, in and around southern China, and in and around the western part of New Guinea, but were less than 60% of the normal in southern Pakistan and southeastern Indonesia (Figure 12). In western Japan, multiple landfall typhoons and active seasonal stationary fronts caused anomalous high precipitation amounts from July to September, resulting in the second-highest monthly precipitation amounts for September since 1946 on the Pacific Ocean side of the country.

2. Tropical cyclones

A total of 25 tropical cyclones (TCs[1]) had formed over the western North Pacific up to September 2018 as compared to the normal of 18.4. The total of 9 TCs forming in August was the second-highest since 1951 (Table 1).

From June to September, a total of 5 TCs with maximum sustained wind speeds of more than 105 knots (classified by RSMC Tokyo as Violent typhoons) made landfall on China, Japan, the Philippines and South Korea.

The most intense of these TCs – Typhoon Mangkhut – formed on September 7 and made landfall on Luzon Island in the Philippines with a maximum wind speed of approximately 110 knots before passing around 100 km south of Hong Kong. According to reporting by the Hong Kong Observatory, extensive circulation and fierce winds associated with Mangkhut on September 16 triggered record storm surges in many places and caused severe flooding in many low-lying coastal areas of Hong Kong, despite the event's temporal proximity to the occurrence of local neap tides.

Notice (11th April, 2019)
Figure 11 and 12 were found to be those for the year 2017. On 11th April 2019, TCC replaced these figures to the correct ones for 2018. Sorry for the inconvenience.

1 Here, a TC is defined as a tropical cyclone with a maximum sustained wind speed of 34 knots or more.

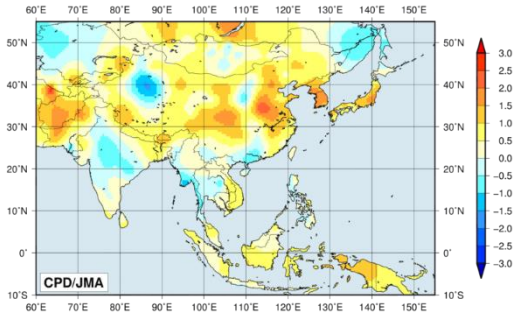

Figure 11 Four-month mean temperature anomalies (°C) from June to September 2018

The base period for normal is 1981 – 2010. Note that the data in Afghanistan, Bhutan, Cambodia, Kazakhstan, Nepal, North Korea, Papua New Guinea, Sri Lanka and Vietnam are interpolated due to the lack of CLIMAT report or climatological normal.

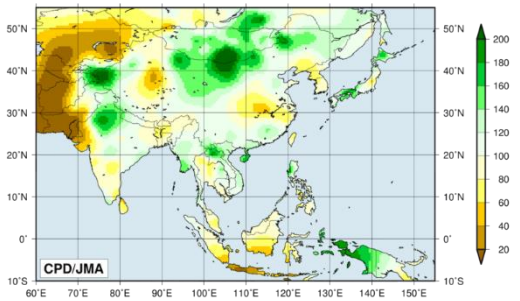

Figure 12 Four-month precipitation ratios (%) from June to September 2018

The base period for normal is 1981 – 2010. Note that the data in Afghanistan, Bhutan, Cambodia, Kazakhstan, Nepal, North Korea, Papua New Guinea, Sri Lanka and Vietnam are interpolated due to the lack of CLIMAT report or climatological normal.

Table 1 Tropical cyclones forming over the western North Pacific up to September 2018

Number ID	Name	Date (UTC)	Category[1)]	Maxumum wind[2)] (knots)
T1801	Bolaven	1/3–1/4	TS	35
T1802	Sanba	2/11–2/13	TS	35
T1803	Jelawat	3/25–4/1	TY	105
T1804	Ewiniar	6/5–6/8	TS	40
T1805	Maliksi	6/8–6/11	STS	60
T1806	Gaemi	6/15–6/17	TS	45
T1807	Prapiroon	6/29–7/4	TY	65
T1808	Maria	7/4–7/11	TY	105
T1809	Son-Tinh	7/17–7/19	TS	40
T1810	Ampil	7/18–7/23	STS	50
T1811	Wukong	7/23–7/27	STS	50
T1812[3)]	Jongdari	7/24–8/3	TY	75
T1813	Shanshan	8/3–8/10	TY	70
T1814	Yagi	8/4–8/13	TS	40
T1815	Leepi	8/11–8/15	STS	50
T1816	Bebinca	8/13–8/17	TS	45
T1817[4)]	Hector	8/13–8/15	TS	40
T1818	Rumbia	8/15–8/18	TS	45
T1819	Soulik	8/16–8/24	TY	85
T1820	Cimaron	8/18–8/24	TY	60
T1821	Jebi	8/27–9/4	TY	105
T1822	Mangkhut	9/7–9/17	TY	110
T1823	Barijat	9/11–9/13	TS	40
T1824[5)]	Trami	9/21–10/1	TY	105
T1825[5)]	Kong-Rey	9/29–10/6	TY	105

Note: Based on information from the RSMC Tokyo-Typhoon Center.
1) Intensity classification for tropical cyclones
TS: tropical storm, STS: severe tropical storm, TY: typhoon
2) Estimated maximum 10-minute mean wind.
3) Date of Typhoon Jongdari includes the period that it was temporally degraded from TC.
4) Typhoon Hector crossed the International Dateline from the East Pacific basin, the date indicates the period that it located in the West Pacific basin.
5) Based on early analysis data, not best track.

3. Monsoon activity and atmospheric circulation

Convective activity (inferred from OLR) averaged for June – September 2018 was enhanced from the Philippines to the Mariana Islands and over northwestern India, and was suppressed from the Indian Ocean to the western part of the Maritime Continent (Figure 13). OLR index data (Table 2) indicate that the overall activity of the Asian summer monsoon (represented by the SAMOI (A) index) was above normal from June to August and was below normal in May and from September to October. The active convection area was shifted northward (SAMOI (N) index) and eastward (SAMOI (W) index) of its normal position from June to August. Strengthened convective activity around the Philippines (Figure 14) was observed several times between June and August, indicating an active Southeast Asian monsoon.

In the upper troposphere (Figure 15 (a)), northeastward extension of the Tibetan High was stronger than normal and anticyclonic circulation anomalies straddling the equator were seen from Southeast Asia to the tropical western Pacific. In the lower troposphere (Figure 15 (b)), cyclonic circulation anomalies were seen from the northern part of the South China Sea to the seas east of the Philippines, indicating a stronger-than-normal monsoon trough over Southeast Asia. Surface westerly winds (Figure 16) were stronger than normal from the southern part of the South China Sea to the Mariana Islands. Zonal wind shear between the upper and lower troposphere over the North Indian Ocean and southern Asia (Figure 17) was stronger than normal from June to August.

(Section 1 and 2: Kenji Kamiguchi, 3: Hiroki Togawa, Climate Prediction Division)

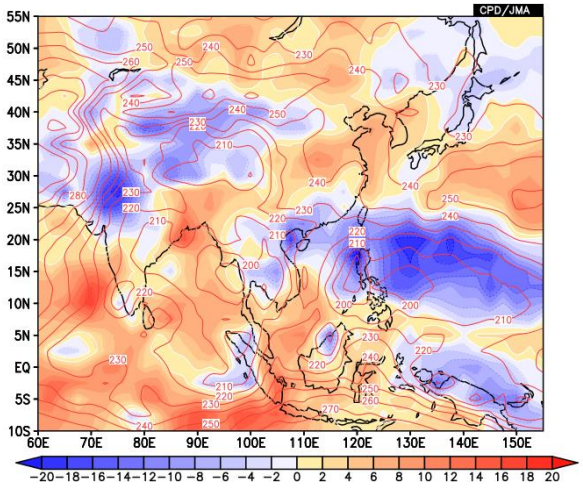

Figure 13 Four-month mean OLR and its anomaly for June–September 2018

The contours indicate OLR at intervals of 10 W/m^2, and the color shading denotes OLR anomalies from the normal (i.e., the 1981–2010 average). Negative (cold color) and positive (warm color) OLR anomalies show enhanced and suppressed convection compared to the normal, respectively. Original data are provided by NOAA.

Table 2 Summer Asian Monsoon OLR Index (SAMOI) values observed from May to October 2018

Asian summer monsoon OLR indices (SAMOI) are derived from OLR anomalies from May to October. SAMOI (A), (N) and (W) indicate the overall activity of the Asian summer monsoon, its northward shift and its westward shift, respectively. SAMOI definitions are as follows: SAMOI (A) = (-1) × (W + E); SAMOI (N) = S – N; SAMOI (W) = E – W. W, E, N and S indicate area-averaged OLR anomalies for the respective regions shown in the figure on the right normalized by their standard deviations.

	Summer Asian Monsoon OLR Index (SAMOI)		
	SAMOI (A): Activity	SAMOI (N): Northward-shift	SAMOI (W): Westward-shift
May 2018	-0.7	-2.2	1.6
Jun. 2018	0.8	1.8	-0.7
Jul. 2018	1.0	0.6	-1.3
Aug. 2018	0.6	2.1	-0.3
Sep. 2018	-1.4	-0.1	-2.0
Oct. 2018	-1.5	-1.0	1.4

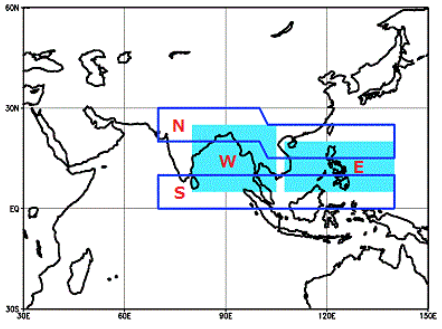

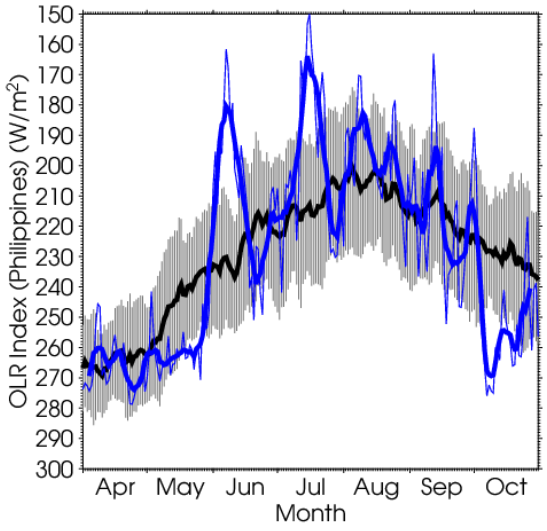

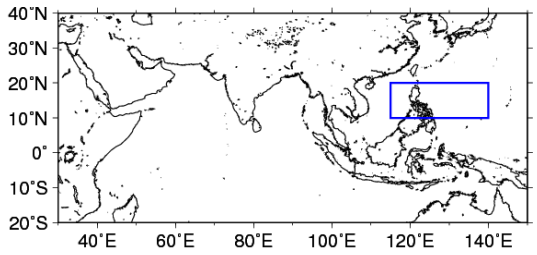

Figure 14 Time-series representation of OLR (W/m^2) averaged over the Philippines (shown by the rectangle on the right: 10°N - 20°N, 115°E - 140°E)

The OLR index is calculated after Wang and Fan (1999). The thick and thin blue lines indicate seven-day running mean and daily mean values, respectively. The black line denotes the normal (i.e., the 1981 - 2010 average), and the gray shading shows the range of the standard deviation calculated for the time period of the normal.

(a)

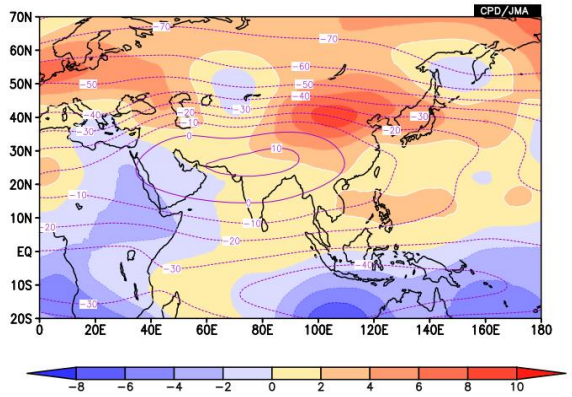

(b)

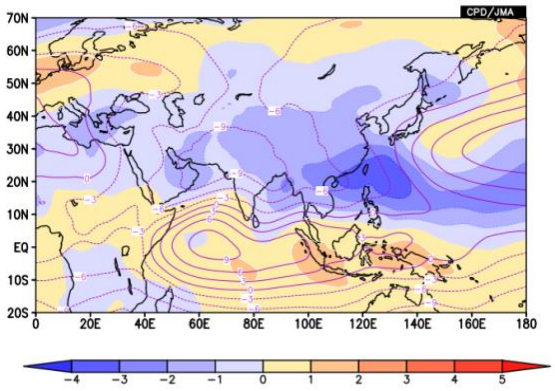

Figure 15 Four-month mean (a) 200-hPa and (b) 850-hPa stream function (contour) and its anomaly (color shading) for June–September 2018

Contour intervals are (a) 10 × 10^6 m^2/s and (b) 4 × 10^6 m^2/s. Warm (cold) shading denotes anticyclonic (cyclonic) circulation anomalies in the Northern Hemisphere, and vice-versa in the Southern Hemisphere. The base period for the normal is 1981 – 2010.

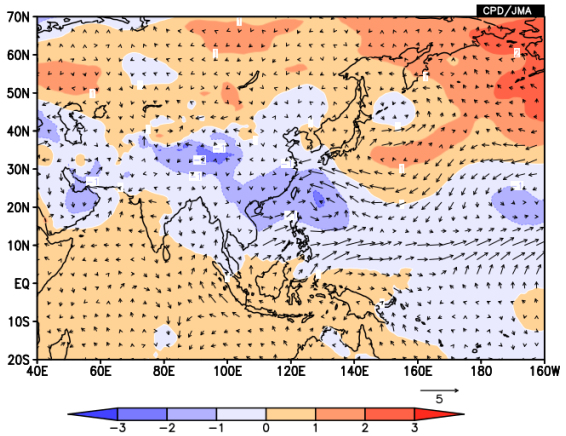

Figure 16 Sea level pressure anomaly (shade) and surface wind vector anomaly (vectors) for June–September 2018.

The shade shows sea level pressure anomalies at intervals of 1 hPa. The base period for the normal is 1981 – 2010.

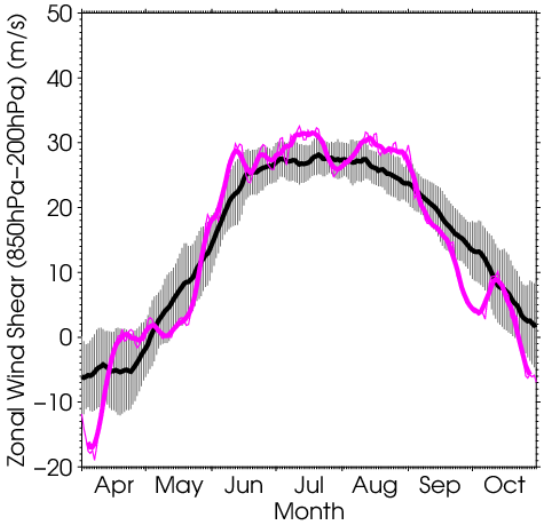

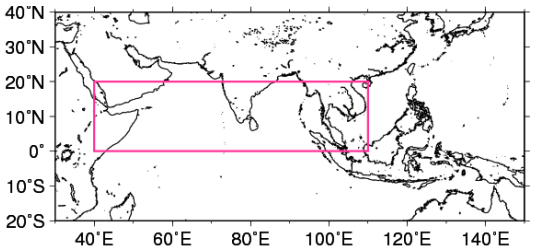

Figure 17 Time-series representation of the zonal wind shear index between 200-hPa and 850-hPa averaged over the North Indian Ocean and southern Asia (the region enclosed by the pink rectangle in the right figure: equator – 20°N, 40°E – 110°E)
The zonal wind shear index is calculated after Webster and Yang (1992). The thick and thin pink lines indicate seven-day running mean and daily mean values, respectively. The black line denotes the normal (i.e., the 1981 – 2010 average), and the gray shading shows the range of the standard deviation calculated for the time period of the normal.

References

Wang, B., and Z. Fan. 1999. Choice of South Asian summer monsoon indices. Bulletin of the American Meteorological Society 80:629–638, http://dx.doi.org/10.1175/1520-0477(1999)080<0629:COSASM>2.0.CO;2.

Webster, P. J. and S. Yang, 1992: Monsoon and ENSO: Selectively interactive systems. *Quart. J. Roy. Meteor. Soc.*, **118**, 877 – 926.

Status of the Antarctic Ozone Hole in 2018

The size of the Antarctic ozone hole in 2018 has exceeded the most recent decadal average due to very cold stratospheric conditions. However, a statistically significant decrease in its maximum size since 2000 is observed.

Since the early 1980s, the Antarctic ozone hole has appeared every year in austral spring with a peak in September or early October. It is generally defined as the area in which the total ozone column value is below 220 m atm-cm.

According to JMA analysis based on data from the Ozone Monitoring Instrument (OMI) on the Aura platform, the Antarctic ozone hole in 2018 appeared in mid-August, expanded rapidly from late August onward, and has developed to become larger than the most recent decadal average (Figure 18, upper left). Its maximum size for the year (observed on 20 September) was 24.6 million square kilometers (see the upper-right panel in Figure 18), which is 1.8 times as large as the Antarctic Continent itself. In 2018, the polar vortex over Antarctica was stable and large, and the stratospheric temperature was much lower than the most recent decadal average after mid-July. This resulted in increased formation of polar stratospheric clouds (PSCs), which play an important role in ozone destruction, and may have contributed to the expanded scale of the year's ozone hole. However, a statistically significant decrease in the maximum size of the Antarctic ozone hole since 2000 has been identified. The report titled *WMO/UNEP Scientific Assessment of Ozone Depletion: 2018* detailed that the hole is expected to close gradually, with spring-time total column ozone in the 2060s returning to 1980 values.

The ozone layer acts as a shield against ultraviolet radiation, which can cause skin cancer. The ozone hole was first recognized in the early 1980s and reached its maximum size of 29.6 million square kilometers in 2000. The Antarctic ozone hole significantly affects summer climatic conditions on the surface of the Southern Hemisphere according to the recent assessment.

(Takanori Matsumoto, Ozone Layer Monitoring Center)

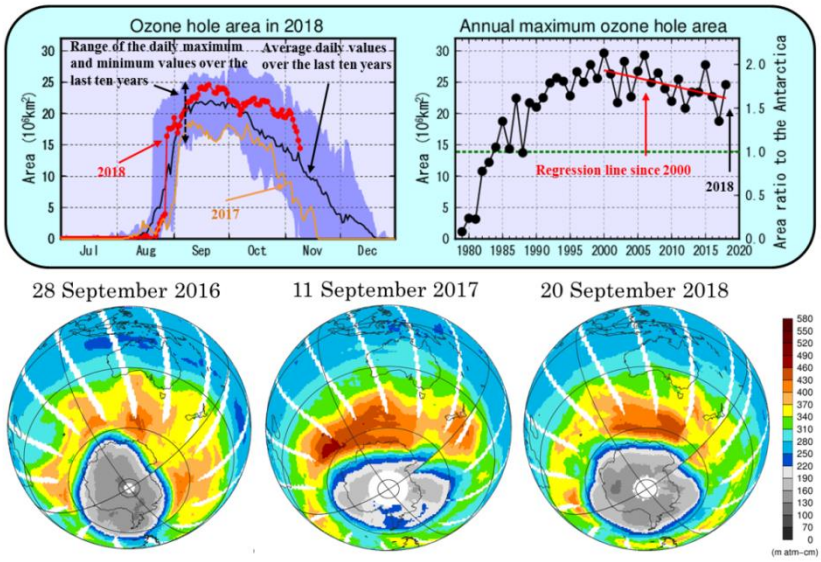

Figure 18 Characteristics of the Antarctic ozone hole

Upper left: Time-series representation of the daily ozone hole area for 2018 (red line) and the 2008–2017 average (black line). The blue shading area represents the range of daily minima and daily maxima over the past 10 years.

Upper right: Inter-annual variability of annual maximum ozone hole area. The green dotted line shows the overall area of the Antarctic Continent (13.9 million square kilometers).

Bottom: Snapshots of total column ozone distribution on the day of the annual maximum ozone hole area for the last three years; the ozone hole is shown in gray (below 220m atm-cm). These panels are based on data from NASA satellite sensors of the Ozone Monitoring Instrument (OMI).

TCC training seminar on One-month Forecast

JMA's Tokyo Climate Center (TCC) has engaged in efforts to help National Meteorological and Hydrological Services (NMHSs) improve their climate services since 2008. The Center's two major activities in this regard involve providing basic climate data, products and tools to NMHSs through its website and assisting with capacity development at NMHSs in the Asia-Pacific region. TCC holds annual training seminars as part of capacity development activities in its role as an RCC in the WMO RA II area. In addition to running annual training seminars, TCC arranges expert visits to NMHSs to promote the effective transfer of technology and discuss the support for climate services.

This time, TCC held the Training Seminar on One-month Forecast from 12 to 16 November 2018 at JMA Headquarters in Tokyo. The event was attended by 15 experts from NMHSs in Bangladesh, Bhutan, Cambodia, Hong Kong (China), Indonesia, Lao People's Democratic Republic, Malaysia, Mongolia, Myanmar, Nepal, Pakistan, the Philippines, Sri Lanka, Thailand and Viet Nam. The seminar focused on improving knowledge about one-month forecast and on enhancing skills in generating one-month forecast products using statistical downscaling methods. The course included lectures and practical exercises using data, products and a web-based application tool available on the TCC website as well as in-situ observation data of attendees' own countries. A new application to be provided online by next March was used in the exercise sessions. The tool was developed to support users' provision of one-month forecast, and valuable feedback to be reflected in the application was collected from attendees ahead of its release. At the end of the seminar, all participants gave presentations on one-month forecast in their own countries for the middle November to early December and engaged in fruitful discussions with lecturers and others present.

The content of the lectures is available on the TCC website at

https://ds.data.jma.go.jp/tcc/tcc/library/library2018.html.

(Atsushi Minami, Tokyo Climate Center)

Attendees on a courtesy visit to JMA Director-General Dr. Toshihiko Hashida (12 November 2018, Director-General's office)

Attendees with JMA Global Environment and Marine Department Director-General Mr. Shogo Tanaka and other JMA staff

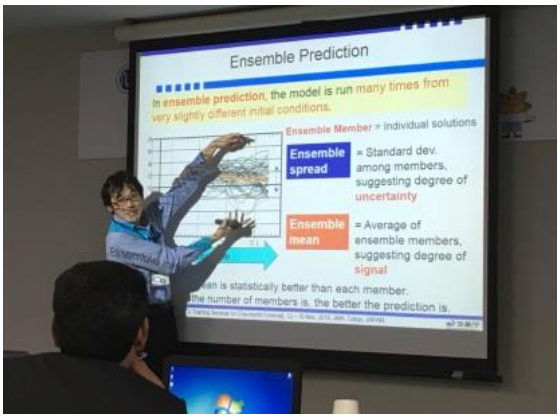

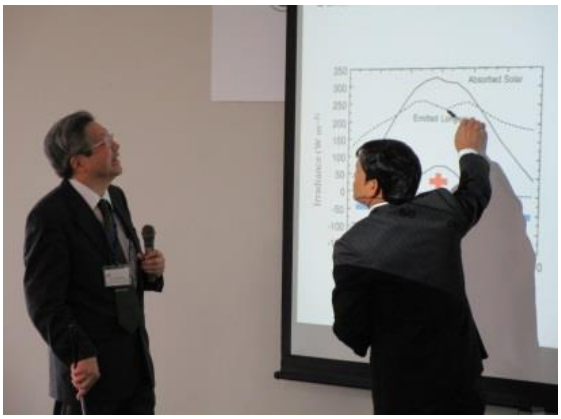

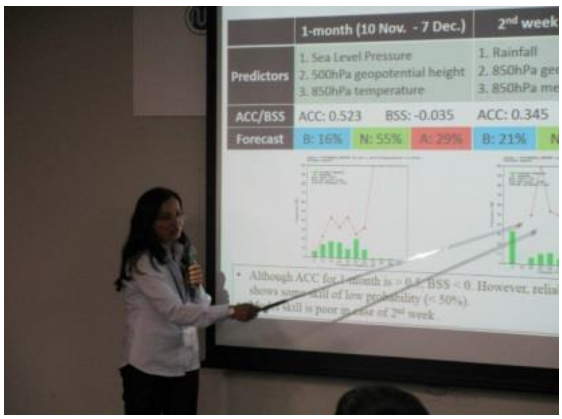

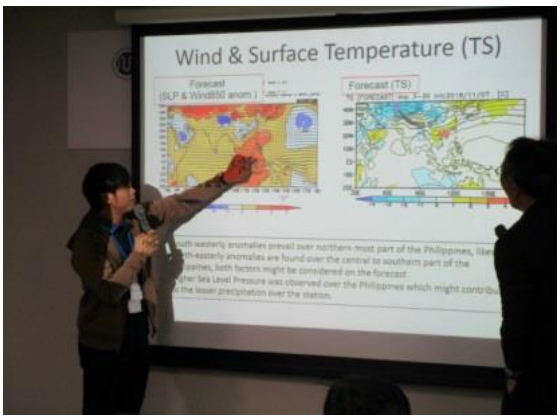

Lectures and practical exercises at the seminar

TCC contributions to Regional Climate Outlook Forums

WMO Regional Climate Outlook Forums (RCOFs) bring together national, regional and international climate experts on an operational basis to produce regional climate outlooks based on input from participating NMHSs, regional institutions, Regional Climate Centers and global producers of climate predictions. By providing a platform for countries with similar climatological characteristics to discuss related matters, these forums ensure consistency in terms of access to and interpretation of climate information.

In autumn 2018, TCC dispatched experts to SASCOF-13, and EASCOF-6.

SASCOF-13

The Sri Lanka Department of Meteorology (DoM) hosted the 13th winter session of the South Asian Climate Outlook Forum (SASCOF-13) from 26 to 28 September 2018 in Colombo, Sri Lanka. The event was supported by the World Meteorological Organization (WMO), the Regional Climate Center (RCC) Pune of the India Meteorological Department (IMD), the UK Met Office (UKMO) and the Regional Integrated Multi-hazard Early-warning System for Africa and Asia (RIMES) with funding from the Asia – Regional Resilience to Changing Climate (ARRCC) program based on UKMO and RIMES collaboration. The 40 or so attendees discussed climatic conditions during the upcoming winter monsoon season (Oct. to Dec. 2018).

As part of the activities of WMO's Global Producing Center for long-range forecasts (GPC-LRF), an expert from GPC-LRF Tokyo provided a winter monsoon season outlook based on JMA's dynamical seasonal ensemble prediction system with probabilistic information on atmospheric variability and the evolution of oceanic conditions in the tropical Pacific and Indian Ocean for the period from Oct. to Dec. 2018. The provision of this information was intended to support the output of country-scale outlooks by National Meteorological and Hydrological Services (NMHSs) in South Asia and contribute to the summarization of a consensus outlook for South Asia.

The forum placed particular emphasis on the Climate Services User Forum (CSUF) with focus on the water sector based on the sharing of information with user sectors to support discussion of their experiences of using climatic services. The GPC-LRF Tokyo expert was also involved in active discussions to promote better use of climate services through future SASCOF activities.

EASCOF-6

The sixth session of EASCOF (EASCOF-6), hosted by the Korea Meteorological Administration (KMA), was held in Seoul in the Republic of Korea from 7 to 9 November 2018. More than 40 experts from China, Japan, Mongolia and the Republic of Korea attended to discuss the heavy rains and high temperatures of this summer and the seasonal forecast for the winter monsoon in East Asia. Discussions also covered recent understandings on climate variations in the East Asian monsoon. Two TCC experts gave presentations on heavy rain and the heatwave seen in the boreal summer of 2018, verification of forecasting for last year's East Asian winter monsoon, the El Niño outlook, and the outlook for the coming winter. Exchanges of expertise at this three-day forum are expected to help develop attendees' understanding of phenomena related to the East Asian monsoon and support improvement of their climate services.

(SASCOF-13: Takuya Komori, Tokyo Climate Center, EASCOF-6: Minako Shiota, Tokyo Climate Center)

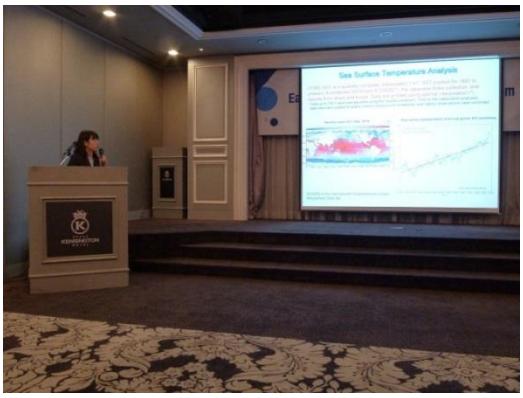

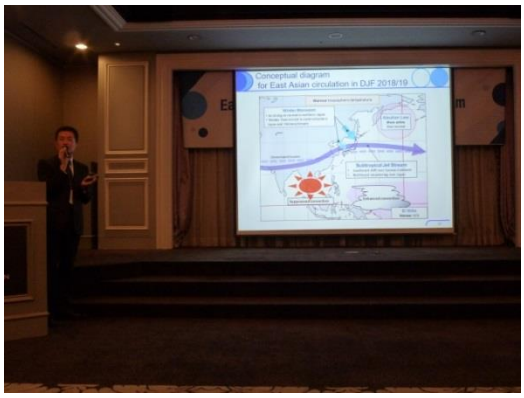

You can also find the latest newsletter from Japan International Cooperation Agency (JICA).

JICA's World (October 2018)

https://www.jica.go.jp/english/publications/j-world/1810.html

JICA's World is the quarterly magazine published by JICA. It introduces various cooperation projects and partners along with the featured theme. The latest issue features "Refugees and Displaced People Rebuilding the Lives of the Displaced".

Any comments or inquiry on this newsletter and/or the TCC website would be much appreciated. Please e-mail to tcc@met.kishou.go.jp.

(Editors: Yasushi Takatsuki, Yasushi Mochizuki and Atsushi Minami)

Tokyo Climate Center (TCC), Japan Meteorological Agency
Address: 1-3-4 Otemachi, Chiyoda-ku, Tokyo 100-8122, Japan
TCC Website: https://ds.data.jma.go.jp/tcc/tcc/index.html